DOI 10.1007/s11595-015-1247-x

A Comparative Study of Different Amorphous and Paracrystalline Silica by NMR and SEM/EDS

JIA Yuan, WANG Baomin*, ZHANG Tingting*
(School of Civil Engineering, Dalian University of Technology, Dalian 116024, China)

Abstract: This work aimed to research the structure models of amorphous materials. Five amorphous and paracrystalline samples (natural or artificial) were investigated via $^{29}Si/^{27}Al$ nuclear magnetic resonance (NMR) and field emission scanning electron microscopy/energy dispersive spectroscopy (FE-SEM/EDS). The results of NMR showed the resonances of different specimens: −93.2 ppm, −101.8 ppm, −111.8 ppm for natural pozzolana opal shale (POS). These peaks were assigned to the Q^2(2OH), Q^3(OH)/Q^4(1Al) and Q^4 respectively. The results of ^{27}Al MAS NMR indicated that Al substituted for Si site in tetrahedral existing in the POS, while the Al/Si atomic ratio in opal was low (around 0.04). For the alkali-silicate-hydrate gel, there were at least three resolved signals assigned to Q^0 and Q^1, respectively. For the fused silica glass powder, there were the primary signals centered about at the range from −107 to −137 ppm, which were assigned to Q^4 units. In addition, the peaks at around −98 and −108 ppm were corresponding to Q^3(1OH) and Q^4 units existing in aerogel silica structure.

Key words: amorphous and paracrystalline silica; the structure models; NMR; Al-substituted

1 Introduction

J B Jones *et al* reported the scanning electron microscopy (SEM) images of the surface of opal firstly[1]. The microstructure of opal was observed directly and showed regular arrangement of nanoscale spheres. Afterwards, many researchers devoted themselves to study the preparation methods of novel silicious materials which possess similar structure of opal, such as aerogel silica. Aerogel silica has many excellent properties: low density, thermal insulation property, high porosity and so on. However, high-cost and cumbersome process of preparation constrain the application of aerogel silica[2-4]. The natural pozzolana opal shale (POS), which contains high percentages of opal sphere, is widely distributed in tertiary lacustrine deposit in China[5]. The silica in POS observed under the SEM and X-ray diffraction (XRD) was opal-A, opal-CT and quartz. Compared with precious opal and aerogel silica, cost of POS is much lower. It can be applied to catalysis as carrier and maintain moisture as cosmetic[6-8].

There are diversities of opals in nature. All of them are divided into two types by XRD: precious opal and common opal. Precious opal is totally composed of the amorphous silicas (opal-A), while there are some microcrystal silica (opal-C/opal-CT) detected by XRD in common opal. Jones and Segnit[9] classified opal into three groups in detail. Opals with XRD pattern similar to α-cristobalite without tridymite were designated as opal-C; Opals which have signals of both microcrystal cristobalite and tridymite were termed as opal-CT. Opals that resemble amorphous silica were affirmed as opal-A[10,11]. Langer and Flörke[12] divided opal-A into two groups, opal-AG for gel-like, and opal-AN

(Received: Oct. 20, 2014; Accepted: May 4, 2015)
JIA Yuan(贾援): Ph D; E-mail: jia132012@126.com
*Corresponding author: WANG Baomin(王宝民): Prof.; Ph D; E-mail: wangbm@dlut.edu.cn; ZHANG Tingting(张婷婷): Ph D; E-mail: 85011313@qq.com
Funded by the the National Natural Science Foundation of China (Nos.51278086 and 51578108), the Program for New Century Excellent Talents in University by Ministry of Education of the People's Republic of China (No.NCET-12-0084), China Petroleum Science and Technology Innovation Fund Research Project (No.2013D-5006-0606), Henan Open and Cooperation Project of Science and Technology (No.142106000023), Liaoning BaiQianWan Talents Program (No.2012921073) and Dalian Plan Projects of Science and Technology (No.2013A16GX113)

for network-or glass-like.Opal-A forms nano-spheres existing in the sample like botryoidal cluster[13]. The opal-CT (disordered α-cristobalite and tridymite) which has flaky texture ranges from 3 to over 10 μm across, however thickness is the nanoscale. Wise *et al*[14] and Flörke *et al*[15] described opal-CT as lepisphere (sphere of blades) or rosette-like. It is noticeable that the trend of lepisphere formation is random and disordered.

The purpose of this study is to characterize the structure models of the different varieties of microcrystal/amorphous silicas detailedly in order to extend the application. ^{29}Si and ^{27}Al nuclear magnetic resonance (NMR) spectra have been one of the effective ways to characterize microcosmic structure of siliceous materials. The standard Q^n notation is used, where Q represents a given silica tetrahedron, and n represents the number of associated Si-O-Si per tetrahedron[16]. Q^0 represents nesosilicate. Q^1 represents chain-end group tetrahedra of dimeric or polymeric silicate units. Q^2 which can be defined as Q^{2P} (the "paired" tetrahedral) and Q^{2B} ("bridging" tetrahedra) represents the middle-chain groups[17,18]. Q^3 and Q^4 represent layer tetrahedra and tectosilicate separately[19,20]. In certain circumstances, intermediate ions, such as Al or Fe, replace Si in the silica polymer but do not destroy the original network. There is the placement of Al in the network in either tetrahedral or octahedral coordination[21]. Morever, in order to verify the result of NMR, energy dispersive spectroscopy (EDS) have been applied to show the elementary composition on the local scale[22-24].

2 Experimental

2.1 Materials

Different amorphous silicious materials chosen for this experiment were from commercial supplier, such as high-purity melted quartz powder, hexagonal silica, alkali-silicate-hydrate gel (A-S-H gel) and natural pozzolana opal shale (POS).

The bulk chemical analysis of the dried POS at 105 for 4 h was as mass%: SiO_2 88.35, TiO_2 0.05, Al_2O_3 2.46, Fe_2O_3 0.91, MgO 0.49, CaO 0.12, Na_2O 2.31, K_2O 0.23 and loss on ignition (LOI) 5.13. Al/Si atomic ratio in POS was 0.052.

2.2 Specimens preparation

2.2.1 Natural amorphous silica preparation

For this study, the natural pozzolana opal shale was used in the experiments after grinding to pass through a 0.074 mm (200 mesh) sieve. Based on the curve of thermo-gravimetric analysis (TGA)(Fig.1) of POS-40, the heating treatment temperature was set at 105, 600, and 1 100 ℃ for 2 h, respectively. POS sample was cut, then polished and affixed on 27×46×1.2 mm glass slides. The surface of the specimen was polished down to a thickness of ca. 0.03 mm in order to make a research by FE-SEM/EDS.

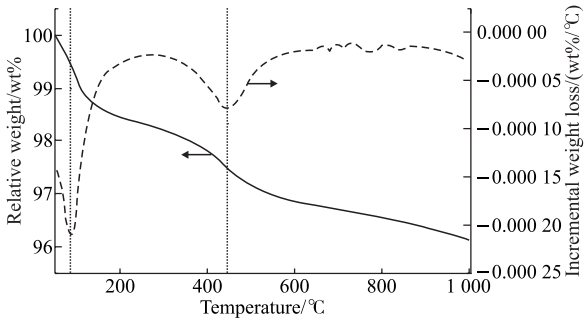

Fig.1 Thermo-gravimetric analysis of natural pozzolana opal shale (POS)

Table 1 Preparation of POS samples with heating temperature

Sample No.	Type of sample	Heating temperature /℃	Heating time/h
POS-40	Particle	40	-
POS-600	Particle	600	2
POS-1100	Particle	1 100	2
POS-S	Slice	25	-

2.2.2 Alkali-silicate-hydrate (A-S-H) gel preparation

Table 2 Batch compositions for aggregate powder reactions

Sample No.	Power weight /g	1 mol/L NaOH /mL	$Al(NO_3)_3$ /g	Al/Si (atomic ratios)
Q	1.27	—	—	—
MQ	1.27	—	—	—
MQ-G	1.27	100	—	—
MQ-A-G	1.27	100	0.89	0.3

Q: quartz powder; MQ: high-purity melted quartz powder; MQ-G: the high-purity melted quartz powder was mixed with NaOH solution; MQ-A-G: the high-purity melted quartz powder and $Al(NO_3)_3$ were mixed with NaOH solution

Alkali-silicate-hydrate (A-S-H) gel preparation was conducted by mixing the high-purity melted quartz powder with sodium hydroxide solution (1 mol/L). Specific compositions for aggregate powder reactions are list in Table 2. NaOH was dissolved in distilled water 24 h prior to mixing, sealed in jars, and stored at room time (25±1 ℃). The pastes were mixed using a magnetic stirring apparatus for 4 h. The fresh sample was poured into plastic bottles of 100 mL. The bottles were sealed, and then stored at room temperature for

100 d. Prior to the analyses, the samples were dried in an oven at 40 ℃ for about 48 h[27].

2.2.3 Aerogel silica preparation

Aerogel silica (AS) was modified by ethyl alcohol (EtOH)/Tri methyl chloro silane (TMCS)/n-hexane solution via ambient pressure drying[28]. After solution exchanging and aging, the wet gels were immersed in EtOH/TMCS/n-hexane solution at 40 ℃ for 48 h. Wang Lijiu *et al*[29] identified the optimum conditions for modification (the mole ratio of EtOH:TMCS=1:1 and the volume ratio of TMCS: wet gels =1:1). The modified wet gels were dried at room temperature for 24 h, then dried in a vacuum drying oven at 50 ℃ for 24 h[30].

2.3 Test methods

Fragments from the specimens of ca. 0.5 cm across were prepared for study under the field emission scanning electron microscope (FE-SEM: NOVA NanoSEM 450)[5]. Samples were attached onto stubs, then coated with gold by the sputter coater for 2 min using 15 mA of electrical current under pressure of 30 Pa. Energy dispersive spectroscopy (EDS) is an important subsidiary component of field emission scanning electron microscopy, which can be used for qualitative and quantitative analysis of the distribution of elements on the micro area of the material in 1 to 3 minutes. The microstructures of samples were determined by FE-SEM, as well as the mole ratio of Al/Si was identified by EDS.

Composites were characterized by $^{29}Si/^{27}Al$ nuclear magnetic resonance (NMR) spectra using a Bruker Avance III 500 MHz spectrometer (field strength of 9.4 T; operating frequency of 79.5 MHz for ^{29}Si and 104.26 MHz for ^{27}Al). Samples were packed into 4mm zirconia rotors and spun at 8 kHz for ^{29}Si and 12 kHz for ^{27}Al. The ^{29}Si and ^{27}Al chemical shifts were referred to external samples of the tetramethylsilane (TMS) and a 1.0 mol/L $AlCl_3 \cdot 6H_2O$ solution, respectively.

3 Results

3.1 ^{29}Si MAS NMR spectra of different amorphous silicious materials

Figs.2 (a, b, c) illustrate the ^{29}Si NMR spectra of the natural pozzolana opal shale at different temperature. The results of NMR spectra are given in Table 3. According to previous study[16], the peaks at around −92 and −101 ppm, are corresponding to $Q^2(2OH)$, $Q^3(OH)$, which are attributed to silicate units in layered structure such as montmorillonite. However, the peak at −101 ppm is assigned to $Q^4(1Al)$ unit too, which is ascribed to Al substituting silicate units in framework structure. The peak at around −111 ppm is attribute to Q^4 unit in framework.

As described by the data in Table 3, the relative intensity of Q^4 unit is between sixty and eighty percent. It illustrates that the structure of opal-A is still framework. With the increase of heat treatment temperature, the relative intensity of $Q^2(2OH)$ site decreases gradually, on the contrary to Q^4 site. Because of dehydroxylation of montmorillonite, $Q^2(2OH)$ and $Q^3(OH)$ sites more into Q^4 site. Moreover, the relative intensity of peak at −102 ppm decreases below 600 ℃, and rises afterward.

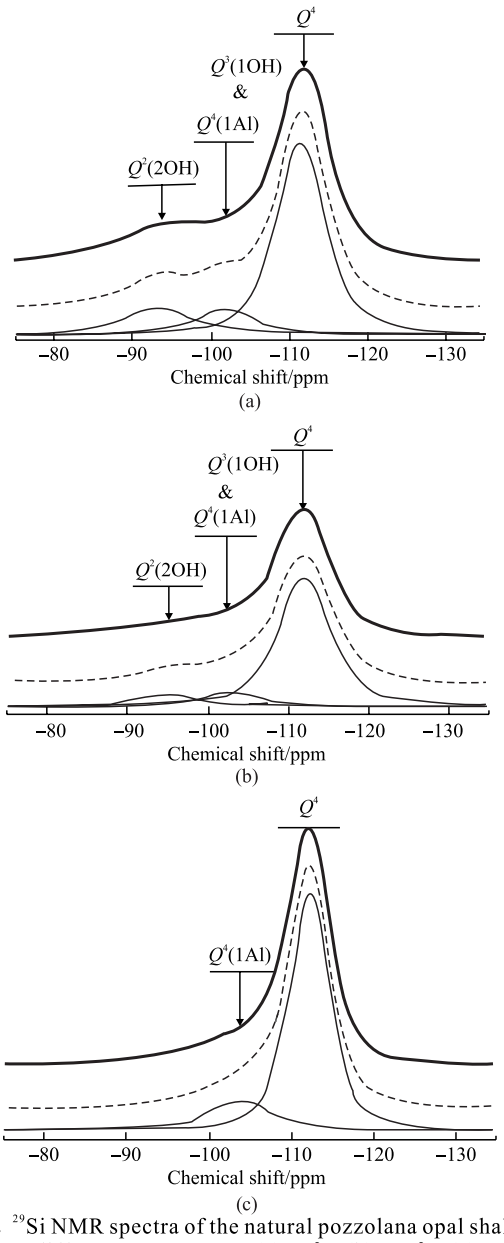

Fig.2 ^{29}Si NMR spectra of the natural pozzolana opal shale at different temperature: (a)40 ℃; (b)600 ℃; (c)1 100℃

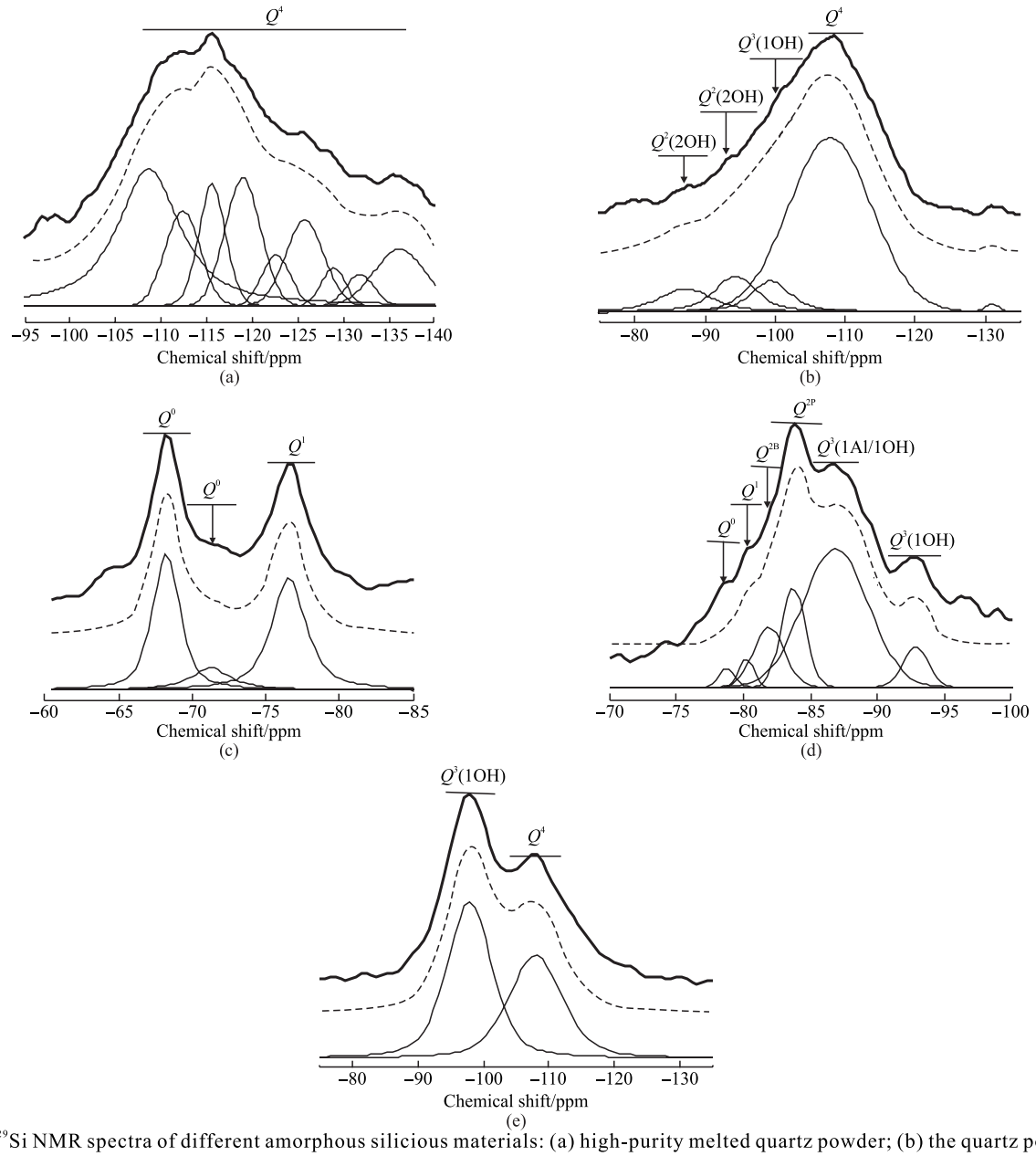

Fig.3 ^{29}Si NMR spectra of different amorphous silicious materials: (a) high-purity melted quartz powder; (b) the quartz powder; (c) the alkali-silicate-hydrate (A-S-H) gel without $Al(NO_3)_3$(MQ-G); (d) alkali-silicate-hydrate (A-S-H) gel with $Al(NO_3)_3$ (MQ-A-G); (e) Aerogel silica (AS)

In order to explore the structure of POS, some natural and artificial amorphous silicas are chosen to compare, such as melted quartz powder, the quartz powder, alkali-silicate-hydrate (A-S-H) gel and aerogel silica(AS). It is observable to identify the differences in the molecule structure of amorphous silicious materials. For the high-purity melted quartz powder (Fig.3(a)) and the quartz powder (Fig.3(b)), there are the primary signals centered about at more than −107 ppm, which are assigned to Q^4 units. Because of high-purity melted quartz is highly-disordered, Q^4 units are differentiated into some small peaks. There are Q^2 and Q^3 existing in quartz sample attributing to mechanical polishing. The polishing process destroys the original frame structure of quartz. For the alkali-silicate-hydrate gel, there are at least three resolved signals centered at −68, −71 and −76 ppm, which are assigned to Q^0 and Q^1 (Fig.3(c)), respectively. However, alkali-silicate-hydrate gel is prepared with $Al(NO_3)_3$ (Fig.3(d)) resulting in structure transformation. Evidently, a few new signals at about −82, −83, −87 and −92.9 ppm appear, which can be attributed to Q^{2B}, Q^{2P}, Q^3(1Al/1OH), and Q^3(1OH) respectively. The transformation indicates that the structure of gel transforms from island to layer due to the increase in the degree of polymerization. The signal in this chemical shift region is assigned to Q^3 attached to aluminum atoms. Fig.3(e) shows the peaks at around −98 and −108 ppm are corresponding to Q^3(1OH) and

Table 3 ^{29}Si NMR spectra data of amorphous silicious materials

Sample No.	Q^n	Centroid/ppm	FWHM/ppm	Gauss+Lor area percentage
POS-40	Q^4	−111.8	7.6	71.4
	Q^3(1OH)/Q^4(1Al)	−101.8	8.4	12.5
	Q^2(2OH)	−93.2	10.2	15.7
POS-600	Q^4	−112.0	7.9	80.2
	Q^3(1OH)/Q^4(1Al)	−102.6	8.4	10.7
	Q^2(2OH)	−95.1	8.4	10.1
POS-1100	Q^4	−112.2	5.9	82.0
	Q^4(1Al)	−104.1	9.3	18.0
	Q^2(2OH)	—	—	—
Q	Q^4	−107.9	13.9	75.4
	Q^3(1OH)	−99.4	6.5	7.6
	Q^2(2OH)	−94.3	7.0	9.5
		−87.2	8.8	7.5
MQ	Q^4	−108.6~ −136.2	—	100
MQ-G	Q^1	−76.6	2.8	46.2
	Q^0	−71.3	3.2	11.6
		−68.2	2.2	42.2
MQ-A-G	Q^3(1OH)	−92.9	2.2	6.8
	Q^3(1Al/1OH)	−86.9	5.7	59.9
	Q^{2P}	−83.7	2.2	16.2
	Q^{2B}	−81.9	2.7	12.4
	Q^1	−80.2	1.3	2.8
	Q^0	−78.8	1.4	2.0
AS	Q^4	−110.2	10.1	47.9
	Q^3(1OH)	−97.9	8.2	52.1

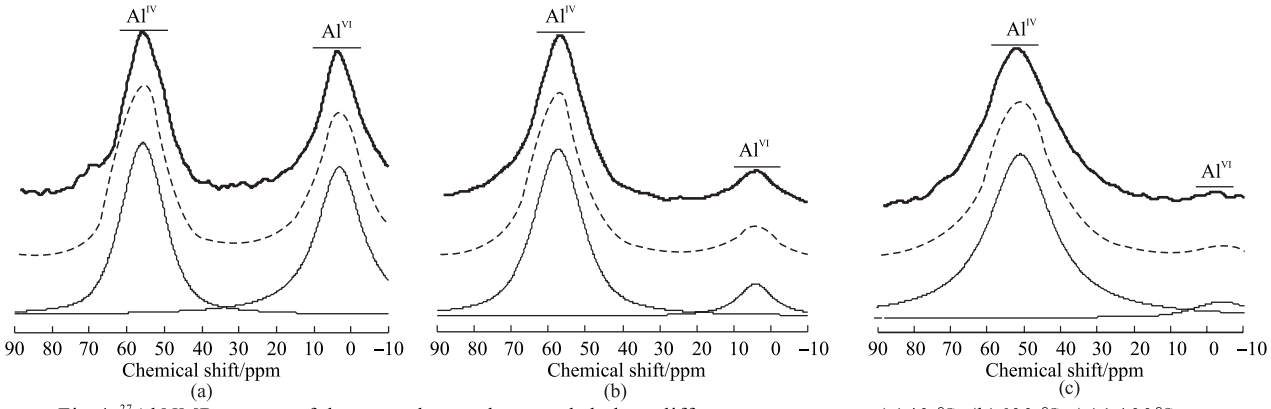

Fig.4 ^{27}Al NMR spectra of the natural pozzolana opal shale at different temperature: (a)40 ℃; (b)600 ℃; (c)1 100℃

Q^4 units existing in aerogel silica structure.

3.2 ^{27}Al MAS NMR spectra of different amorphous silicious materials

According to previous studies[31], four-fold coordinated(Al^{IV}) is revealed by shifts from 50 to 80 ppm, while six-fold coordinated(Al^{VI}) is indicated by shifts from −10 to 20 ppm. The resulted ^{27}Al NMR spectra of POS are shown in Fig.4. There are two resonances: one signal at about 55 ppm and the other at 3 ppm. With the increase of temperature, the intensity of six-fold coordinated peak decreases sharply, even

Table 4 ^{27}Al NMR spectra data of amorphous silicious materials

Sample No.		Centroid /ppm	FWHM /ppm	Gauss+Lor area percentage
POS-40	Al_O	3.1	14.6	51.9
	Al_T	55.7	13.8	48.1
POS-600	Al_O	4.0	11.4	13.9
	Al_T	57.4	15.4	86.1
POS-1100	Al_O	-4.1	17.6	6.6
	Al_T	51.0	20.9	93.4
MQ-A-G	Al_T	59.0	6.6	100.0

Table 5 Calculated value of Al/Si atomic ratio on the basis of NMR

Sample No.	Al/Si atomic ratio
POS-40	0.035
POS-600	0.027
POS-1100	0.047
MQ-A-G	0.249

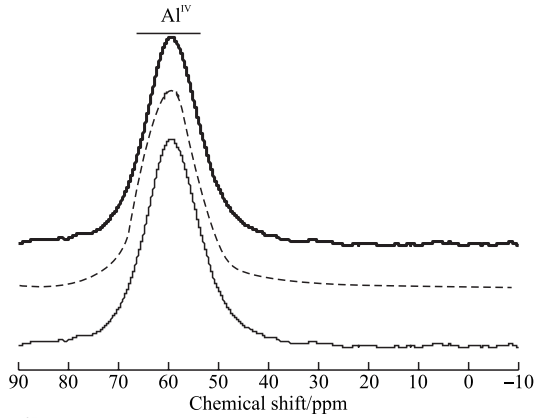

Fig.5 ^{27}Al NMR spectra of the alkali-silicate-hydrate (A-S-H) gel with $Al(NO_3)_3$(MQ-A-G)

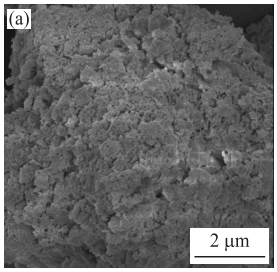

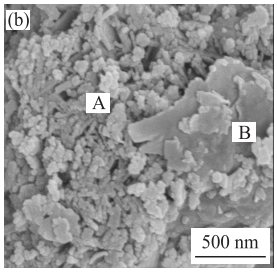

Element	Weight/%	Atomic%
O	43.08	42.56
Al	0.88	0.52
Si	22.30	12.55
C	33.73	44.38
Total	100	100

Element	Weight/%	Atomic%
O	41.20	38.58
Al	2.35	1.31
Si	12.67	6.76
C	42.39	52.87
Mg	0.21	0.13
K	0.33	0.13
Fe	0.85	0.23
Total	100	100

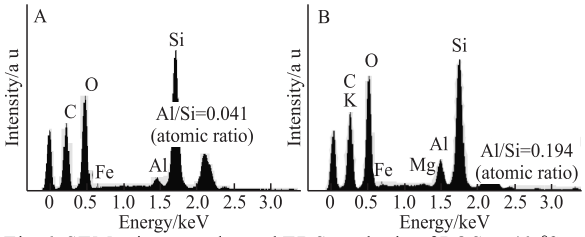

Fig.6 SEM micrographs and EDS analysis of POS at 40 ℃: (a)40 000×; (b)160 000×(C: $CaCO_3$, O: SiO_2, Mg: MgO, Al: Al_2O_3, Si: SiO_2, K: MAD-10 Feldspar, Fe: Fe)

disappears finally. For the alkali-silicate-hydrate gel with $Al(NO_3)_3$ (MQ-A-G, Fig.5), the ^{27}Al NMR spectra display a single resonance around 59 ppm. The result establishes that Al ions substituting for silicon atoms are all in a tetrahedral arrangement[16].

According to the data of ^{29}Si NMR spectra, Al/Si atomic ratio in tetrahedron can be obtained with the following equations via the deconvolution area[25,26].

Natural pozzolana opal shale:

$$Al/Si=\frac{0.25\ Q^4(1Al)}{Q^3+0.75Q^4(1Al)} \quad (1)$$

Alkali-silicate-hydrate (A-S-H) gel :

$$Al/Si=\frac{1/3\ Q^3(1Al/10H)}{Q^0+Q^1+Q^2+Q^3(1OH)+2/3Q^4(1Al/10H)} \quad (2)$$

3.3 FE-SEM and EDX analysis

Fig.6 and Fig.7 show the SEM micrographs of POS particles at 40 and 1 100 ℃ separately. POS particles are covered with a mass of amorphous SiO_2 (Fig.6(a)). When the magnification gets to 160 000×, some schistose particles are found between spheres (Fig.6(b)). After heat treatment, amorphous SiO_2

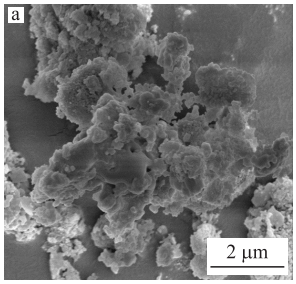

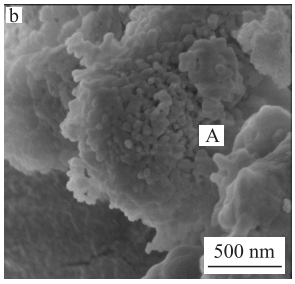

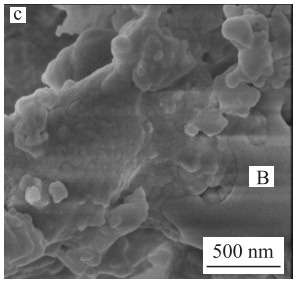

Element	Weight/%	Atomic%
O	53.04	62.2
Al	1.41	0.98
Si	38.4	25.65
C	7.15	11.17
Total	100	100

Element	Weight/%	Atomic%
O	48.02	52.03
Al	4.14	2.66
Si	19.06	11.76
C	20.98	30.28
Mg	0.66	0.47
K	2.37	0.74
Fe	4.77	2.06
Total	100	100

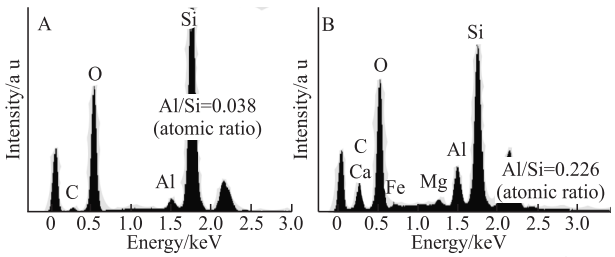

Fig.7 SEM micrographs and EDS analysis of POS at 1 100 ℃: (a)40 000×; (b)160 000×; (c)160 000×(C: $CaCO_3$, O: SiO_2, Mg: MgO, Al: Al_2O_3, Si: SiO_2, Ca: Wollastonite, Fe: Fe)

spheres fuse and interact with each other(Figs.7(a,b,c)). According to the EDS energy spectrum analysis of amorphous SiO_2 spheres and schistose particles, different testing data were obtained. Amorphous SiO_2 spheres have low Al/Si atomic ratio (0.04), while schistose particles have higher Al/Si atomic ratio (0.19-0.23). This is contrast to previous studies[16], which indicates that there is little Al for Si substitution. The schistose particle might be montmorillonite grain. The data of EDS shows that schistose particles are montmorillonite possiblly, which demonstrates the reason for the increase of Al/Si atomic ratio.

4 Discussion

Both natural pozzolana opal shale and aerogel silica are frame structures. They have relatively parallel structure. However, there is a disparity in percentage of Q^3 and Q^4 units. Aerogel silica consists of a large number of independent spheres with Si-OH on the surface, while the opal-A particles of POS interact with each other resulting in the decrease of Q^3(OH). Opal-A and opal-CT are the major silica minerals of POS. Langer and Flrke[11] divided opal-A into non-crystalline opal-AN (net-work-like) and opal-AG (gel-like). The former was natural silica glass which was transported by water steam and deposited on the volcanic rocks[16] and the latter was an aggregate of non-/micro-crystalline silica particles which was formed at relatively low temperatures[4,8,32]. It is very difficult to distinguish opal-AN and opal-AG under conventional detection devices, such as IR, XRD and SEM. According to NMR data, it is obvious that the atomic structure of POS differs from high-purity melted quartz powder which is typically glassy. The atomic structure of the glassy material is more complex due to the effect of high temperature. The characteristic of melted quartz is short-range order and long-range disorder leading to the dissociation of Q^4 unit. The opal-A sphere of POS is more likely to belong to opal-AG. Quartz whose main resonance is -107 ppm for Q^4 is typical crystal, which is hardly detected on POS under NMR in contrast with the result of XRD. It is illustrated that the content of quartz is rare, although quartz in POS is crystallized well.

Compared with the network structure of aerogel silica, alkali-silicate-hydrate (A-S-H) gel without Al^{3+} is island structure. After Al^{3+} is added in the A-S-H gel, nesosilicates structure transforms into layer structure. Al^{3+} plays a key role in chaining free silicon-oxygen tetrahedral together. Fig.5 shows Al ions take the place of Si sites completely. The calculated value of A-S-H gel with Al^{3+} under NMR is approximately 0.249. In the alkali-silicate system, Al^{3+} can be involved in the gel easily. On the contrary, Fig.6 and Fig.7 indicate opal-A contain as much as 0.04 (Al/Si molar ratio). It is in contract to some previous studies[16,33], which reported little or no Al for Si substitution in opals.

Table 5 shows that the calculated value of Al/Si atomic ratio of POS without thermal treatment is approximately 0.035, which is close to the Al/Si atomic ratio of opal-A spheres. Actually, the value contains the content of Q^3(1OH) and Q^4(1Al). With the increase of temperature, montmorillonite disintegrates gradually and aluminium-oxygen octahedron transforms into aluminium-oxygen tetrahedron. Because Al substituting for Si unit can not happen under 1 100 ℃, transformation quantity can not detected by ^{29}Si NMR. When the temperature is over 1 100 ℃, Al starts to substitute Si due to the fusion of POS. This is the reason for the increase of calculated value of Al/Si atomic ratio.

5 Conclusions

The natural pozzolana opal shale is composed of non- or micro-crystal, quartz and montmorillonite. Opal-A is non-crystal and opal-CT is micro-crystal. Frame work represents the structure of opal-A and opal-CT. Moreover, montmorilllonite is layer structure and aluminium-oxygen octahedron can transform into aluminium-oxygen tetrahedron under heating at 1 100 ℃. The atomic structure model of opal-A which is interconnected gel-state sphere cluster, is consistent with aerogel silica. On the contrary, there is great difference in the structures of opal-A and A-S-H gel/ melted quartz. In alkaline environment, Al^{3+} can substitute for Si in ASH gel easily. The result of the detection validates that Al ions substituting for silicon atoms can occur in the diagenetic process. However, the replacement rate is low. The content of Al in opal-A is 0.04.

References

[1] Jones J B, Sanders J V, Segnit E R. Structure of Opal[J]. *Nature*, 1964, 204: 990-991

[2] Akitt J W, Greenwood N N, Lester G D. Nuclear Magnetic Resonance and Raman Studies of the Aluminium Complexes formed in Aqueous Solutions of Aluminium Salts containing Phosphoric Acid and Fluoride Ions[J]. *Journal of chemical society(A)*, 1971: 2 450-2 457

[3] Wang L J, Zhao S Y. Synthesis and Characteristics of Mesoporous Silica Aerogels with One-step Solvent Exchange/Surface Modification[J]. *Journal of Wuhan University of Technolotgy-Mater. Sci. Ed*., 2009, 24(4): 613-618

[4] Kureti S, Weisweiler W. A Novel Sol-gel Method for the Synthesis of c-Aluminium Oxide: Development of the Sol-gel Transformation and Characterization of the Xerogel[J]. *Journal of Non-Crystalline Solids*., 2002, 303(2): 253-261

[5] Ren L F. The Discovery and Research of Light Shale Compose of Cristobalite and Tridymite[J]. *Bulletin of the Chinese Ceramic Society.,* 1982 (2): 13-17

[6] Liu Y, Zheng SL, Du GX, *et al.* Photocatalytic Degradation Property of Nano-TiO_2/Diatonite for Rodamine B Dye Wastewater[J]. *International Journal of Modern Physics B*, 2009, 23: 1 683-1 688

[7] Zheng S L, Bai C H, Gao R Q. Preparation and Photocatalytic Property of TiO_2/Diatomite-based Porous Ceramics Composite Materials[J]. *International Journal of Photoenergy*, 2012, 10:1-4

[8] Sun Z M, Bai C H, Zheng S L, *et al.* A Comparative Study of Different Porous Amorphous Silica Minerals Supported TiO_2 Catalysts[J]. *Applied Catalysis A: General.* 2013, 458: 103-110

[9] Jones J B, Segnit E R. The Nature of Opal I. Nomenclature and Constituent Phases[J]. *Journal of the Geological Society Society of Australia*, 1971, 18:57

[10] Graetsch H, Gies H I, Topalovi. NMR, XRD and IR Study on Microcrystalline Opals[J]. *Phys. Chem. Minerals*, 1994, 21(3): 166-175

[11] Onal M, Kahraman S, Sarikaya Y. Differentiation of a-Crisrobalite from Opals in Bentonites fromTurkry[J]. *Applied Clay Science,* 2007, 35: 25-30

[12] Langer K, Flörke O W. Near Infrared Absorption Spectra(4 000-9 000 cm^{-1}) of Opals and The Role of "Water" in these $SiO_2{\cdot}nH_2O$ Mineral[J]. *Fortschrift Der Miner*, 1974, 52:17-51

[13] Saminpanya S, Sutherland F L. Silica Phase-Transformations During Diagenesis Within Petrified Woods Found in Fluvial Deposits from Thailand-Myanmar[J]. *Sedimentary Geology*, 2013,290: 15-26

[14] Wise J R, Kelt K. Inferred Diagenetic History of a Weakly Silicified Deep Sea Chalk[J]. *Gulf Coast Association of Geological Societies Transactions*, 1972, 22: 177-203

[15] Flörke O W, Jones J B, Segnit E R. Opal-CT Crystals[J]. *Neues Jahrbuch fur Mineralogie Monatshefte*, 1975,8: 369-377

[16] Brown L D, Ray A S, Thomas P S. ^{29}Si and ^{27}Al NMR Study of Amorphous and Paracrystallin Opals from Australia[J]. *Journal of Non-Crystalline Solids*, 2003, 332(1-3): 242-248

[17] Dai Z, Tran T T, Jorgen S. Aluminum Incorporation in the C-S-H Phase of White Portland Cement-Metakaolin Blends Studied by ^{27}Al and ^{29}Si MAS NMR Spectroscopy[J]. *Journal of the American Ceramic Socirty,* 2014, 97(8): 2 662-2 671

[18] Hu C G, Hu S G, Ding Q J, *et al.* Effect of Curing Regime on Degree of Al^{3+} Substituting for Si^{4+} in C-S-H Gels of Hardened Portland Cement Pastes[J]. *Journal of Wuhan University of Technology-Mater. Sci. Ed.,* 2014, 29(3): 546-522

[19] Gross A F, Le V H, Kirsch B L, *et al.* Correlations between Silica Chemistry and Structural Changes in Hydrothermally Treated Hexagonal Silica/Surfactant Composites Examined by *in situ* X-ray Diffraction[J]. *Chem. Mater*., 2001,13(10): 3 571-3 579

[20] Graetsch H, Gies H, Topalovic I. NMR, XRD and IR Study on Microcrystalline Opals[J]. *Physics and Chemistry of Minerals*, 1994, 21(3): 166-175

[21] Hinman N W, Kotler J M. Aluminum in Silica Phases Formed in Hot Springs[J]. *Procedia Earth and Planetary Science*, 2013, 7: 365-368

[22] Fritsch E, Gaillou E, Rondeau B, *et al.* The Nanostructure of Fire Opal[J]. *Journal of Non-crystalline Solids*, 2006, 352(38-39): 3 957-3 960

[23] Wang C L, Zheng S L, Liu G H, *et al.* Preparation of Wollastonite Coated with Nano-aluminium Silicate and Its Application in Filling PA6[J]. *Surface Review and Letters,* 2010, 17: 265-270

[24] Sun Z M, Zheng L M, Zheng S L, *et al.* Preparation and Characterization of TiO_2/acid Leached Serpentinite Tailings Composites and Their Photocatalytic Reduction of Chromium(VI) [J]. *Journal of Colloid and Interface Science*, 2013, 8(404): 102-109

[25] Baasner A, Schmidt B C, Webb R L. Fluorine Speciation as a Function of Composition in Peralkaline and Peraluminous Na_2O-Glasses: A Multinuclear NMR Study[J]. *Geochimica et Cosmoclumica Acta*, 2014, 132: 151-169

[26] Maruyama I, Nishioka Y, Matsui G K. Microstructural and Bulk Property Changes in Hardened Cement Paste During the First Drying Process[J]. *Cement and Concrete Research*, 2014, 58: 20-34

[27] Gwenn L S, Mohsen B H H, Frank W, *et al.* Hydration Degree of Alkali-activated Slags: A ^{29}Si NMR Study[J]. *The American Ceramic Society*, 2011, 94: 4 541-4 547

[28] Ma H N, Wang B M, Zhao L, *et al.* Preparation and Properties of PMMA Modifi ed Silica Aerogels from Diatomite[J]. *Journal of Wuhan University of Technology-Mater. Sci. Ed*., 2014.29(5): 877-884

[29] Wang L J, Zhao S Y. Synthesis and Characteristics of Mesoporous Silica Aerogels with One-step Solvent Exchange/Surface Modification[J]. *J. Wuhan University of Technology -Mater. Sci. Ed*., 2009, 24(4): 613-618

[30] Shi F, Wang L J, Liu J X. Synthesis and Characterization of Silica Aerogels by a Novel Fast Ambient Pressure Drying Process[J]. *Mater. Lett.*, 2006, 60(29-30): 3 718-3 722

[31] Dressler M, Nofz M, Malz F, *et al.* Aluminum Speciation and Thermal Evolution of Aluminas Resulting from Modified Yoldas Sols[J]. *Journal of Solid State Chemistry*, 2007, 9(180): 2 409-2 419

[32] Jessica M E, Stephen B R. Tem and X-ray Diffraction Evidence for Cristobalite and Tridymite Stacking Sequences in Opal[J]. *Clays and Clay Minerals*, 1996, 4(44): 492-500

[33] Francois B, Bittencourt R D, Robert M D, *et al.* Role of Aluminum in the Structure of Brazilian Opals[J]. *Eurpean Journal of Mineralogy,* 1990, 5(2): 611